

Article

# Do Artificial Neural Networks Always Provide High Prediction Performance? An Experimental Study on the Insufficiency of Artificial Neural Networks in Capacitance Prediction of the 6H-SiC/MEH-PPV/Al Diode

Andaç Batur Çolak <sup>1</sup>, Tamer Güzel <sup>2</sup>, Anum Shafiq <sup>3</sup> and Kamsing Nonlaopon <sup>4,\*</sup>

<sup>1</sup> Mechanical Engineering Department, Niğde Ömer Halisdemir University, Niğde 51240, Turkey; andacatur.colak@mail.ohu.edu.tr

<sup>2</sup> Mechatronic Department, Niğde Ömer Halisdemir University, Niğde 51200, Turkey; tamerguzel@ohu.edu.tr

<sup>3</sup> School of Mathematics and Statistics, Nanjing University of Information Science and Technology, Nanjing 210044, China; anum\_shafiq@nuist.edu.cn

<sup>4</sup> Department of Mathematics, Khon Kaen University, Khon Kaen 40002, Thailand

\* Correspondence: nkamsi@kku.ac.th

**Abstract:** In this paper, we study a new model that represents the symmetric connection between capacitance–voltage and Schottky diode. This model has a symmetrical shape towards the horizontal direction. In recent times, works conducted on artificial neural network structure, which is one of the greatest actual artificial intelligence apparatuses used in various fields, stated that artificial neural networks are apparatuses that proposal very high forecast performance by the side of conventional structures. In the current investigation, an artificial neural network structure has been generated to guess the capacitance voltage productions of the Schottky diode with organic polymer edge, contingent on the frequency with a symmetrical shape. Of the dataset, 130 were grouped for training, 28 for validation, and 28 for testing. In order to evaluate the effect of the number of neurons on the prediction accuracy, three different models with different neuron numbers have been developed. This study, in which an artificial neural network model, although well-trained, could not predict the output values correctly, is a first in the literature. With this aspect, the study can be considered as a pioneering study that brings a novelty to the literature.

**Keywords:** artificial neural network; MEH-PPV; capacitance–voltage; Schottky diode; barrier height



**Citation:** Çolak, A.B.; Güzel, T.; Shafiq, A.; Nonlaopon, K. Do Artificial Neural Networks Always Provide High Prediction Performance? An Experimental Study on the Insufficiency of Artificial Neural Networks in Capacitance Prediction of the 6H-SiC/MEH-PPV/Al Diode. *Symmetry* **2022**, *14*, 1511. <https://doi.org/10.3390/sym14081511>

Academic Editors: Ji-Huan He and Muhammad Nadeem

Received: 27 June 2022

Accepted: 22 July 2022

Published: 23 July 2022

**Publisher's Note:** MDPI stays neutral with regard to jurisdictional claims in published maps and institutional affiliations.



**Copyright:** © 2022 by the authors. Licensee MDPI, Basel, Switzerland. This article is an open access article distributed under the terms and conditions of the Creative Commons Attribution (CC BY) license (<https://creativecommons.org/licenses/by/4.0/>).

## 1. Introduction

Due to its capabilities in the delicate symmetry of a human brain learning, artificial neural network systems (ANN) have become the topic of many researchers and studies today. This ANN model features a symmetrical structure that runs along the flow direction. Aside from current research into the ANN system's limits and possibilities, its application areas are expanding by the day. The ANN system functions in a manner similar to that of neurons [1]. There are artificial neurons that mimic nerve cells. These neurons typically function as a multi-input, single-output nonlinear element [2]. By connecting them, they construct multi-layer perceptron neural networks. These layers produce outputs based on the algorithm used following a procedure comparable to the learning process [3]. The ANN system's unique operation has provided them with opportunities in a variety of fields. The ability of these systems to generate false data, as well as their success in forecasting non-linear data, has enabled them to be used in a wide range of applications, ranging from health to energy and electronics [4–8]. Metal–semiconductor contacts is one of these areas. Metal–semiconductor interactions have been regarded as a watershed moment in the evolution of electronics science since their introduction. A physical barrier among metal and semiconductor has provided humans with numerous chances in electron control [9].

Many electrical circuit elements based on this arrangement, known as the Schottky barrier, have been constructed [10–12]. The most essential of these are diodes. Diodes are widely employed in today's electronics. Schottky diodes, based on silicon carbide (SiC), are one type of these diodes [13]. The capacity of these diodes to operate in harsh environments distinguishes them from regular diodes [14,15]. The area of application of diodes is directly proportional to their electrical characteristics. As a result, the ANN system may have a significant role to play in establishing the electrical properties of these diodes. At this point, it is critical to evaluate the ANN system's applicability in this field or to discover the boundaries of its potential.

## 2. Literature Review

According to the literature, the uses of the ANN system on Schottky diodes appear to be highly successful due to the analytical data gained from diode measurements. Lim et al. constructed an ANN neural network to assess the inference accuracy of gated Schottky diodes. They observed that when the outputs of artificial neural network are compared with the outputs of test devices, the ANN system can classify with very high accuracy [16]. Rabehi et al. [17] proposed a novel approach for estimating the Schottky diode characteristics with improved precision. They proved that the parameters of the Schottky diode may be correctly computed using a novel function algorithm. Mellit et al. [18] established a simple ANN model for modeling and predicting the power generated by a polycrystalline Schottky diode photovoltaic module. They demonstrated that the suggested model can accurately forecast module output power. M. Alade [19] calculated the electrical characteristics of GaN Schottky diodes at high temperatures using an ANN system. He contrasted the system's outputs to theoretical calculation findings. He demonstrated that the calculated and theoretical findings are in good agreement. Darwish et al. [20] announced an efficient method for calculating current–voltage outputs with the ANN system. They stated that the ANN system's simulation findings demonstrate a clear and perfect fit with the experimental data. They demonstrated that the ANN technique can be utilized to effectively predict the current–voltage at the p–n junction. Mittal et al. [21] studied the ANN system's applicability in analyzing the performance of photovoltaic Schottky diodes. They built a network model since current–voltage is the output. They evaluated the experimental photovoltaic diode output to the ANN system output and the data they collected and discovered that the results were highly consistent. Liang et al. [22] studied the ANN system's availability in the construction of shottky barrier diodes. They used the ANN model to examine the diode's nonlinear power features. According to this investigation, the experimental settings and ANN results agreed well. Torun et al. [23] modeled the I–V characteristic of an Au/Ni/n-GaN/undoped GaN Schottky diode with different machine learning tools. The current values were measured for the voltages applied to the diode terminal of the previously produced Au/Ni/n-GaN/undoped GaN Schottky diode in the range of 40–400K with 20K steps. Using 5192 experimental samples, four dissimilar structures were developed. The performance results of the models were compared with each other. The study results showed that the Adaptive Neuro Fuzzy System can accurately model the I-V characteristics for all temperature values.

Rahman et al. [24] used an ANN model to predict the oscillation heat transport coefficient of a thermoacoustic heat exchanger. Using experimental data, the ANN model for a floating thermoacoustic refrigerator oscillating heat exchanger was built. The MLP network comprises two input parameters and a hidden layer with ten optimum neurons. The collected outcomes established the ANN model's high accuracy prediction ability. Pang et al. [25] focused on creating an ANN model to predict solar radiation. The ANN model was trained using real meteorological data from a nearby weather station. The data collected from the constructed ANN model were compared to the target data, and the model's accuracy was evaluated. The results show that ANN model may produce prediction data that are highly congruent with the target data.

According to the wide research assessment, ANNs show great prediction performance in all studies published in the literature. The key motivation for this study is that all of the studies on ANNs in the literature indicate good predictive capacity of ANNs and no studies on prediction failure of ANN models are discovered in the literature. For the first time, an application in which an ANN model failed was reported in this study. The revised ANN model, which was designed to predict the capacitance–voltage measurement of a diode with an organic polymer interface based on frequency, had exceptionally high error rates and failed to anticipate the target data. The core causes of the failure of the ANN model, which is said to be a mathematical instrument with very good prediction ability, have been carefully explored and debated in all of the research in the literature. This work, which reports the failure of the ANN model for the first time in the literature, is significant since it covers several gaps and is the first study reported on the issue in the literature.

### 3. Experimental Model

An n-type 6H-SiC wafer with a diameter of 2 inches (001) and a donor density of  $2.610^{17} \text{ cm}^{-3}$  was used to fabricate the 6H-SiC/MEH-PPV/Al Schottky diode. After the SiC wafer surface was cleaned with the cleaning technique known as the RCA process, it was kept in HF/H<sub>2</sub>O (1:10) mixture for 20 s to lift the oxide layer shaped on the surface. After this procedure, 150 nm thick pristine gold (99.995%) was evaporated on the polished surface of the semiconductor at  $10^{-6}$  Torr pressure. The Au/SiC wafer was annealed at 500 °C for 5 min to form back contact in the metal evaporation system. Then, Poly[2 -methoxy-5-(2-ethylhexyloxy)-1,4-phenylenevinylene] (known name MEH-PPV) dissolved in toluene was plated with a spin coater at 2000 rpm for 1 min to form an interface polymer layer on the Au/n-SiC wafer surface. The plated wafer was annealed at 60 °C for 5 min to eliminate toluene from the n-6H-SiC surface. Finally, 140 nm thick pristine aluminum (99.999%) was evaporated onto the matte surface of the SiC wafer to form the Schottky contact. The schematic diagram of the experimentally produced 6H-SiC/MEH-PPV/Al Schottky diode is seen in Figure 1. Keithley 2400 Sourcemeter (Tektronix, Inc. Beaverton, OR 97077 United States) was used for current–voltage (I–V) measurements. Current–voltage was made in the voltage range between −3 and +3 V.

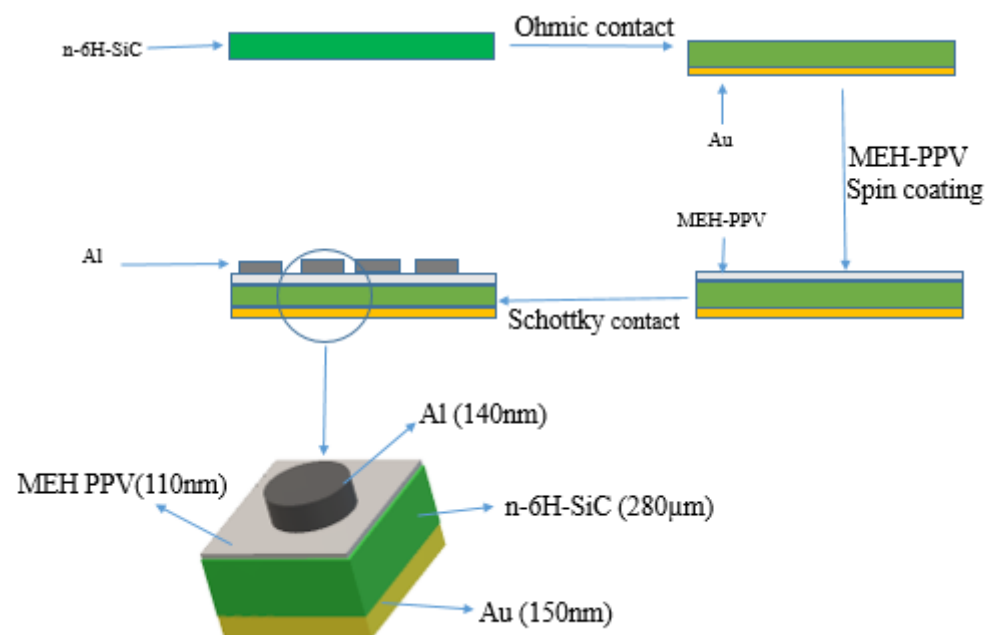


**Figure 1.** Schematic diagram of 6H-SiC/MEH PPV/Al Schottky diode.

#### 4. ANN Model Development

There are numerous mathematical tools in the literature that academics utilize for data processing and modeling [26–30]. Traditional approaches for constructing simulation models utilizing data are shown to be insufficient in several circumstances, such as nonlinear function modeling and irregularity [31]. Artificial intelligence (AI)-based prediction models have recently become tools regularly utilized by academics in various fields. AI-based prediction relies on simulation modeling once the system has been trained with data. Artificial neural networks (ANN) are a prominent AI technique among researchers [32]. According to the literature, ANN models have advantages like straight routes in the learning phase of nonlinear correlations, the ability to move analogue and digital data together, its strong structure even in the presence of noisy input data, the convenience of reusing information thanks to feedback, and high sensitivity in learning new data [33]. ANN models with various structures exist, including the radial basic functional neural network (RBFNN) [34], the convolutional neural network (CNN) [35], and the multi-layer perceptron (MLP) [36]. The MLP network model is the most commonly used of these models. There is at least one hidden layer in MLP networks, in addition to an input and output layer. The MLP network's hidden layer contains computational units known as neurons. Each link between layers is assigned a weight. Signals travelling across each link between layers are multiplied by the weight assigned to that link. By summing the inputs from the neurons in the next layers, a bias is added, and the outcome is achieved by employing a transfer function to acquire the value in the output layer. A connection is produced between nonlinear rules derived from input data and output data in an MLP network using a feed-forward (FF) back-propagation (BP) technique. The MLP network is trained in the FF stage by updating biases and weights. During the training phase, data from the input layer is fed forward and errors are back-propagated by adjusting the weights between neurons. The training phase of ANN model continues in this manner until the lowest error rate is obtained, at which point the training phase of the ANN model is finished.

In this study, an ANN model has been developed to predict the capacitance voltage outputs of an organic polymer interface 6H-SiC/MEH-PPV/Al diode depending on the frequency. The first step in developing ANN models is optimizing and ideally grouping the data. Next comes the determination of hyperparameters such as the number of neurons, hidden layers, training, and transfer algorithms. After the data set and hyperparameters are determined ideally, the model is trained by entering data into the model. After verifying that the training phase is ideally completed, the predictive performance of the model is analyzed. After the ANN model with the highest prediction performance is determined, the implementation phase is started, and the prediction values are obtained from the model. The flowchart of the ANN development methodology is given in Figure 2.

The voltage (V) and frequency (F) values in the input layer of the MLP network model, which has been developed with a total of 186 data, have been defined as input parameters and the capacitance (C) value has been predicted at the output layer. Optimizing the data used in training ANNs is one of the important parameters that directly affects the prediction performance of ANN. For this reason, optimum data grouping has been preferred by making different data optimizations. The data used in the development of ANN are grouped in three separate sections, as frequently preferred in the literature [37–39]. Overall, 70% of the dataset was used for training, 15% for validation, and 15% for testing. Matlab program was used in the development of ANN models. The basic configuration structure of the developed ANN model is shown in Figure 3.

One of the main parameters influencing ANN prediction performance is the number of neurons employed in the hidden layers. For determining the number of neurons to be employed in ANN models, there is no standard modeling or computation technique [40]. As a consequence, three separate ANN models with 5, 10, and 15 neurons in the hidden layers have been built to compare the performance of models developed with varying neuron numbers. The Levenberg–Marquardt method, one of the strongest algorithms often utilized by academics, was used as the training algorithm in the constructed ANN

model [41]. Tan-Sig functions were employed as the transfer function in the MLP network's hidden layer, and Purelin functions were used in the output layer. The transfer functions employed are as follows:

$$f(x) = \frac{1}{1 + \exp(-x)} \quad (1)$$

$$\text{purelin}(x) = x \quad (2)$$

In order to evaluate the prediction performance of the created ANN model, some parameters should be investigated. The Mean Square Error (MSE) and Coefficient of Determination (R) parameters were utilized to examine the performance of the MLP network for this purpose. The rate of variation between the projected values from the ANN model and the target values was also investigated. The equations utilized to compute performance parameters are listed below [42]:

$$\text{MSE} = \frac{1}{N} \sum_{i=1}^N (X_{\text{exp}(i)} - X_{\text{ANN}(i)})^2 \quad (3)$$

$$R = \sqrt{1 - \frac{\sum_{i=1}^N (X_{\text{exp}(i)} - X_{\text{ANN}(i)})^2}{\sum_{i=1}^N (X_{\text{exp}(i)})^2}} \quad (4)$$

$$\text{Error Rate (\%)} = \left[ \frac{X_{\text{exp}} - X_{\text{ANN}}}{X_{\text{exp}}} \right] \times 100 \quad (5)$$

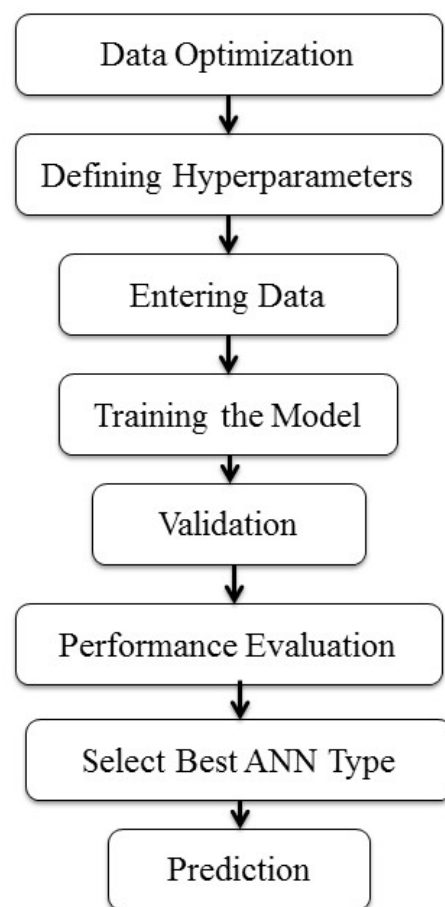


**Figure 2.** The flowchart of the ANN development methodology.

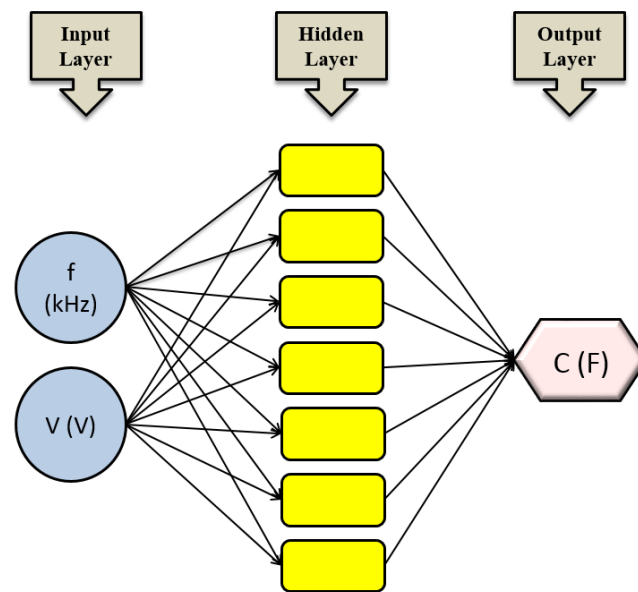


Figure 3. The basic configuration structure of the developed ANN model.

## 5. Results and Discussion

Figure 4 depicts a capacitance–voltage graph of the 6H-SiC/MEH-PPV/Al diode at 50–1000 kHz and room temperature. Figure 4 shows that when the frequency increases, the capacitance value increases as well. However, it has been reported in the literature that as frequency increases, capacitance reduces [43]. This could be owing to the presence of the MEH-PPV polymer at the interface. Because current conduction might be affected by the conductive polymer layer at the interface. This could have influenced the recorded diode capacitance value. Reddy [44] demonstrated that the conductive polymer layer at the interface can influence the diode’s capacitance value.

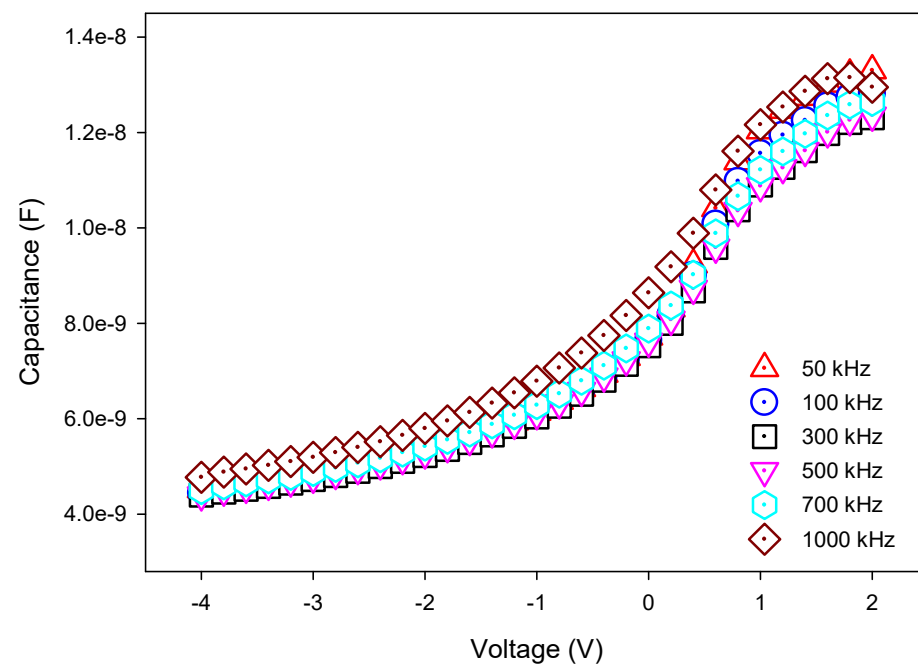


Figure 4. Capacitance–voltage graph of the 6H-SiC/MEH-PPV/Al diode.

Figures 5–7 exhibit data graphs for each stage of the ANN models developed with 5, 10, and 15 neurons, respectively. While the graphs have target values on the x-axes, the y-axes include ANN predictions. The dotted line represents the equality line, while the

solid color lines represent the fitted data values. The objective of these graphs is to assess and demonstrate the proximity of ANN outputs to target values, as well as the error rates between them. When the studies on ANN in the literature are analyzed, it is clear that ANN is a powerful mathematical tool capable of making high-accuracy predictions. The fitted data and the equality line are very near and compatible in the figures derived from these investigations, yet the data points are positioned on or very close to both lines. When the equality line, fitted line, and data points provided in graphics for the data obtained from each stage of the ANN model are closely inspected, the discrepancy between data is readily visible. There is a clear difference between the trends of the equality line and fitted line in each of the graphics. Despite this, the distance and mismatch of data points from both lines are also apparent. In order to determine the accuracy of the ANN, it is important to examine the R values calculated for the model. The ANN model's prediction accuracy is directly proportional to the proximity of the R values to the 1 value. When the studies on ANN undertaken by researchers in the literature are evaluated, it is discovered that the R values are quite close to 1 and positive. When the R values generated for each stage of the ANN model established in this work are reviewed, a situation that differs from the situation in the literature emerges. The distances of the values from 1 are seen when the R values acquired from each built ANN model are inspected. The numerical values of R values reveal that each ANN model's prediction performance is quite low, and it can produce predictions with large inaccuracy.

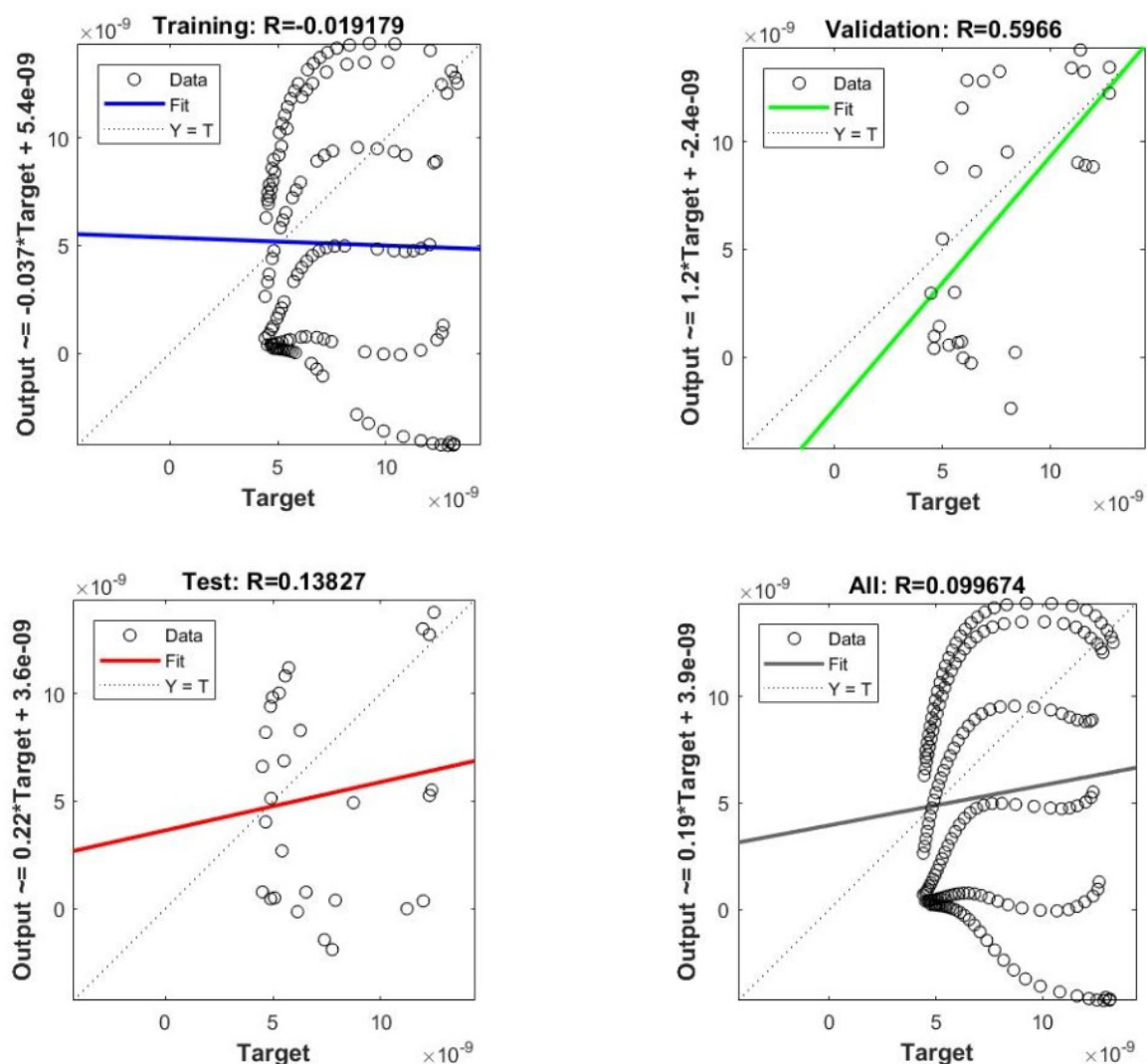


Figure 5. Performance of the ANN for all stages for neuron number 5.

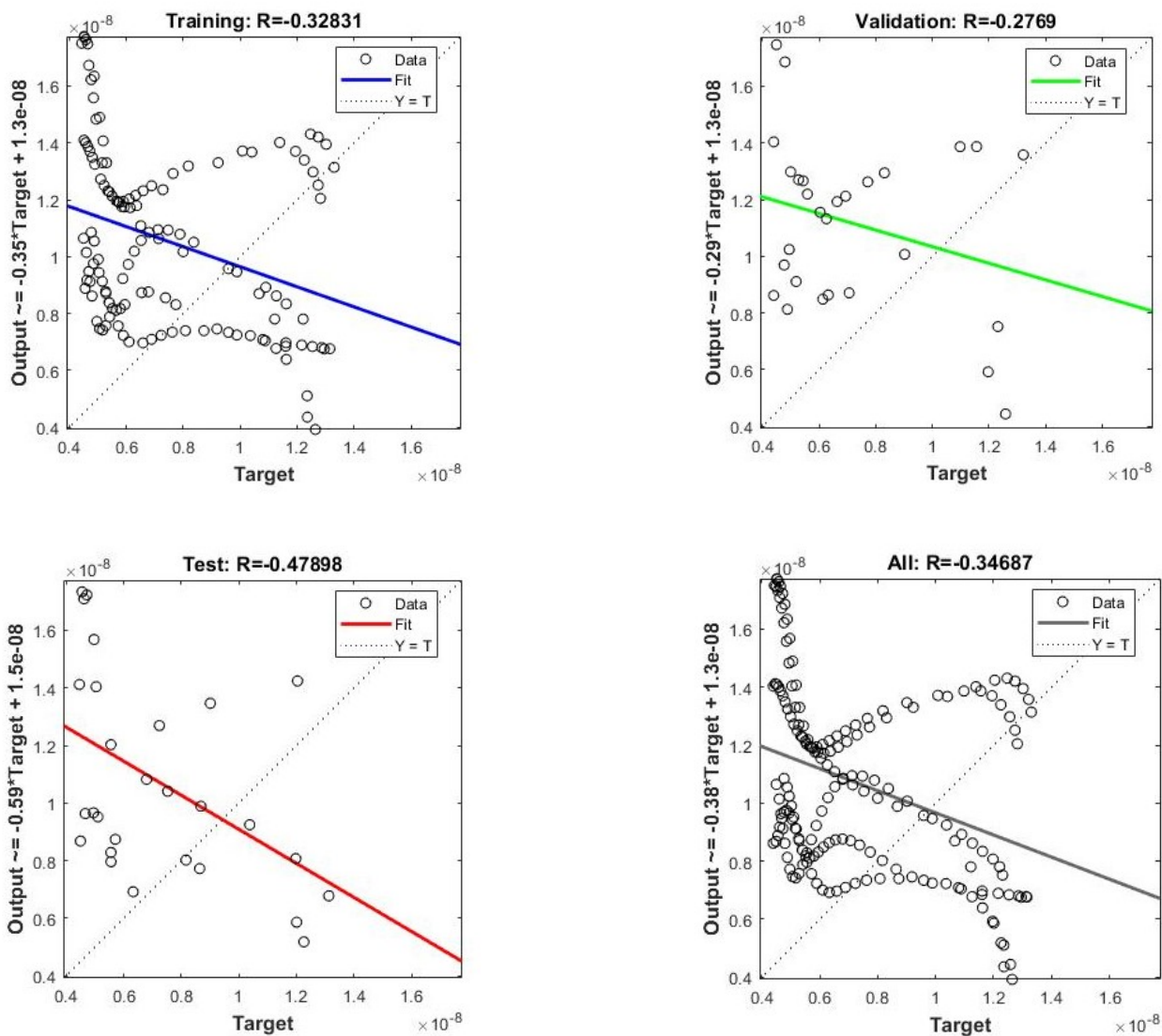


Figure 6. Performance of the ANN for all stages for neuron number 10.

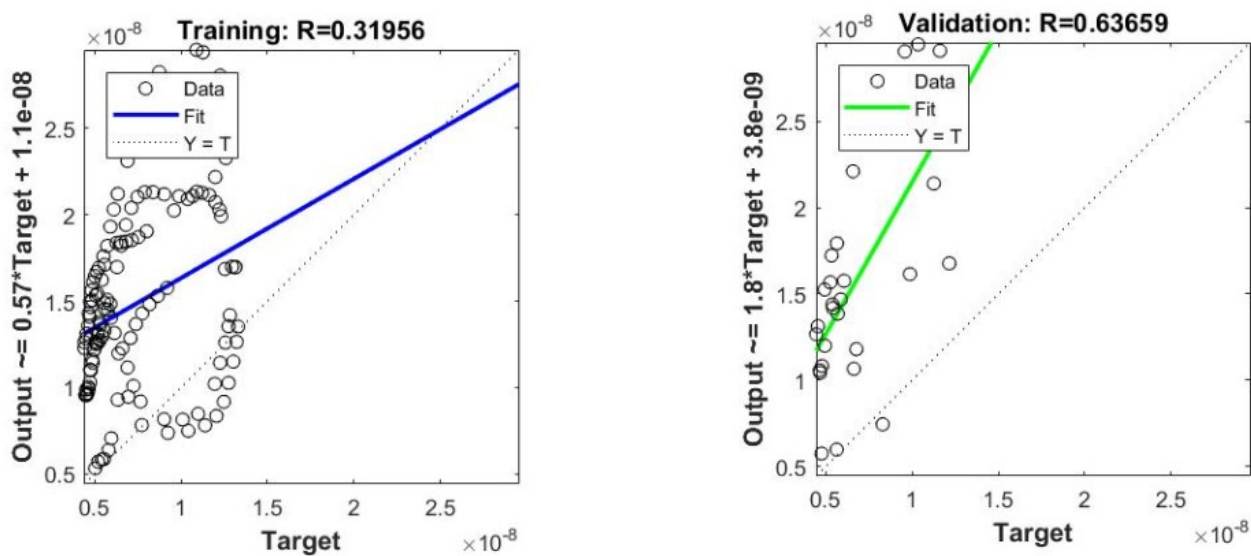


Figure 7. Cont.

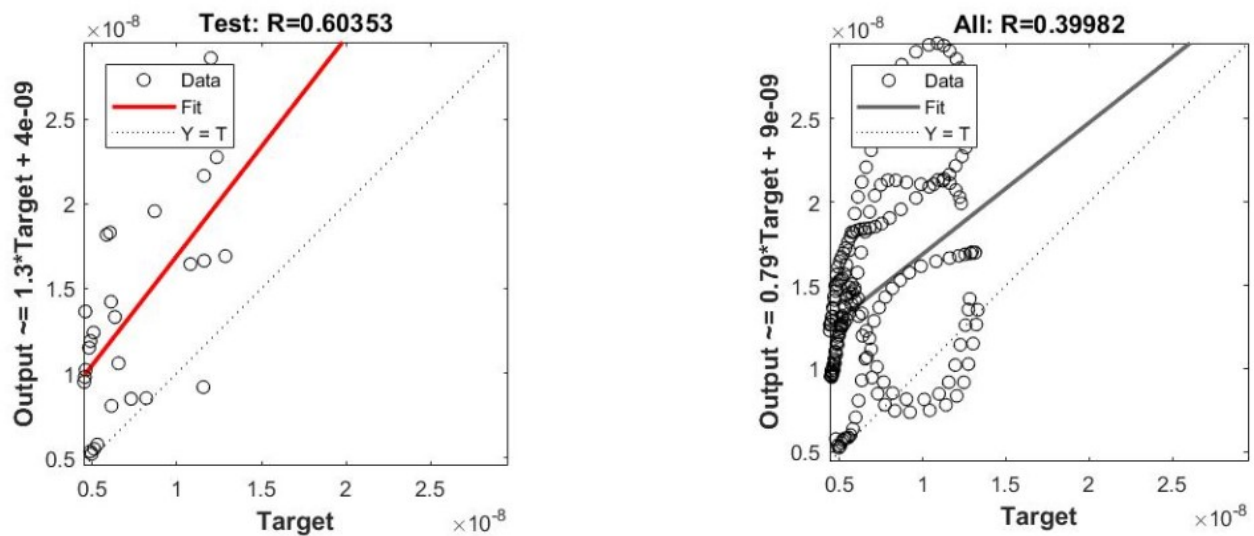
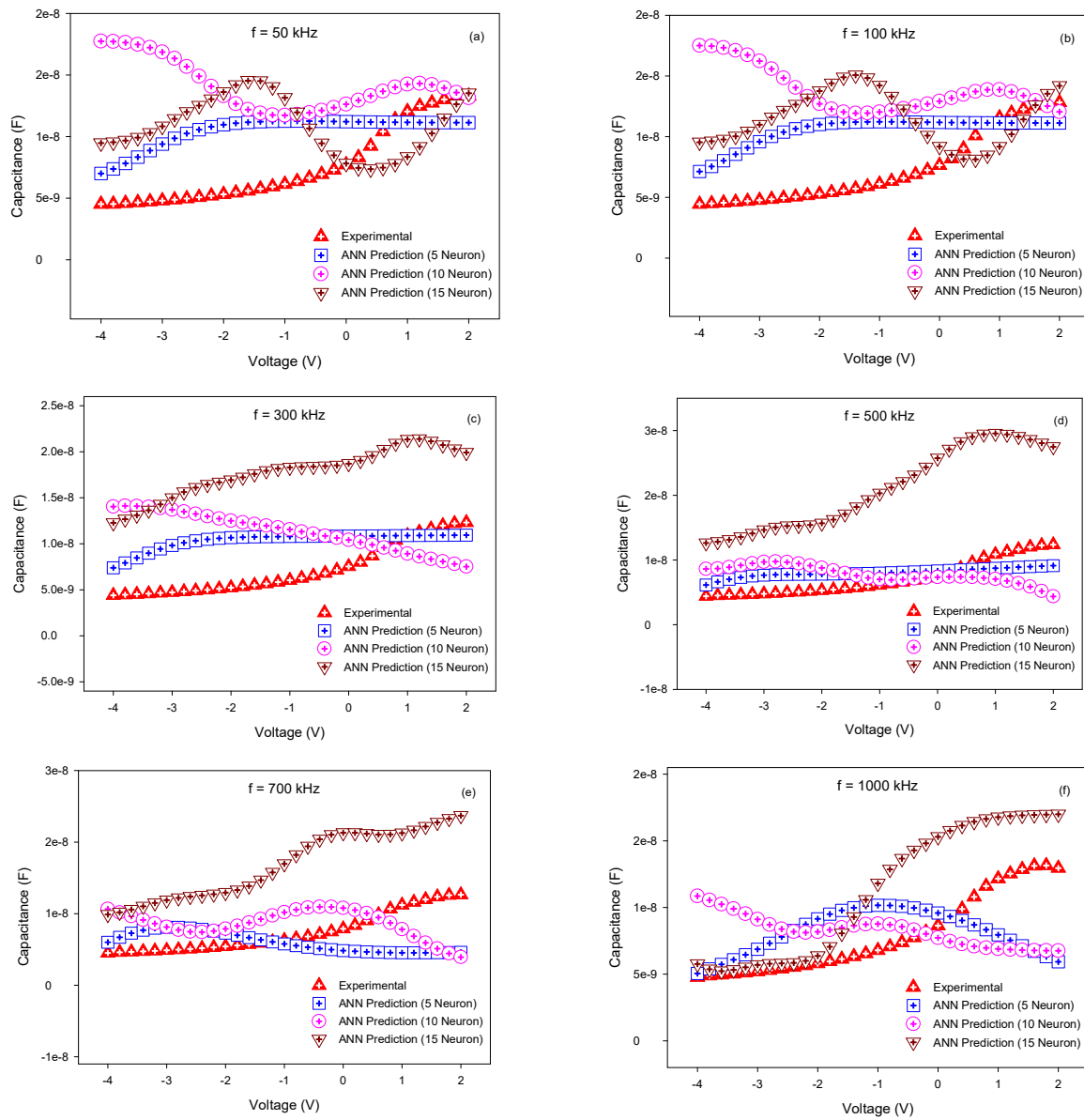


Figure 7. Performance of the ANN for all stages for neuron number 15.

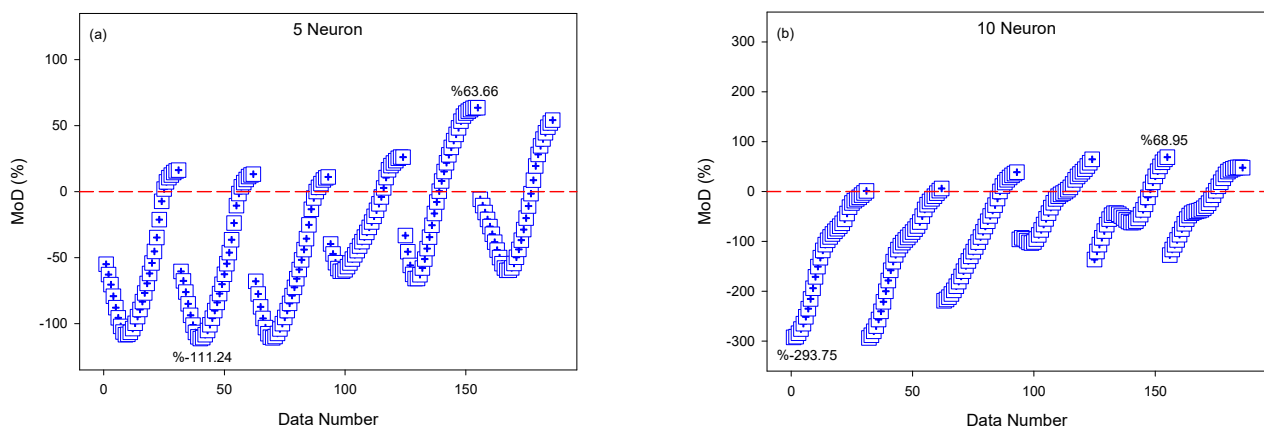
Figure 8 depicts experimental data and ANN predictions on the same graph. Whereas the x-axes of the graphs show voltage levels, the y-axes show capacitance values. The changes in capacitance values at the fixed frequency with regard to the voltage are displayed in separate graphs for each frequency value. The goal of displaying these graphs is to highlight the disparity between ANN predictions and target values. When similar figures in the literature are analyzed, it is discovered that goal values and ANN estimation data are positioned on or extremely close to each other. The closeness of ANN predictions to target values implies that the ANN model delivers accurate predictions. Figure 8 shows that the data points acquired from the ANN model and the goal data points are incompatible and positioned at extremely different positions. When the trends of data lines are indexed, however, there are noticeable variances and mismatches in trend trends. These results reveal that the created ANN model fails to forecast the capacitance voltage outputs of the 6H-SiC/MEH-PPV/Al diode with an organic polymer interface dependent on frequency.

Figure 9 shows the error rates between data from the ANN model and the goal values for each data point. When the error rates of ANN models described in the literature are analyzed in depth, it is discovered that generally low values are produced, and data points are positioned near the zero error line. The close proximity of the data points to the zero error line indicates that the constructed ANN model can make accurate predictions. When Figure 9 is inspected, it is evident that the data points are distant from the zero error line. These exceedingly high error rates indicate that there are exceptionally high error rates between the projected values generated from the constructed ANN model and the target values.

Figure 10 depicts the anticipated and target values from the ANN model on the same graph. The graph shows experimental data with target values on the x-axis and predictive values from the ANN model on the y-axis. The closer the data points are to the equality line depicted in blue, the lower the error rates of the ANN model. When the data from the studies on ANN models undertaken by researchers in the literature is evaluated, it is discovered that the data points are clustered around the equality line. The findings of the research suggests that ANN models can generate accurate predictions. However, when the data from the ANN model developed in this work is examined, it is clear that the location of the data points is unrelated to the equality line. When these data are studied, the failure of the ANN model, which was built to forecast the capacitance voltage outputs of the 6H-SiC/MEH-PPV/Al diode with organic polymer interface dependent on frequency, is plainly visible. Table 1 shows the calculated performance parameters for the created ANN model.



**Figure 8.** Experimental data and ANN predictions. (a) 50 kHz (b) 100 kHz (c) 300 kHz (d) 500 kHz (e) 700 kHz (f) 1000 kHz.



**Figure 9.** Cont.

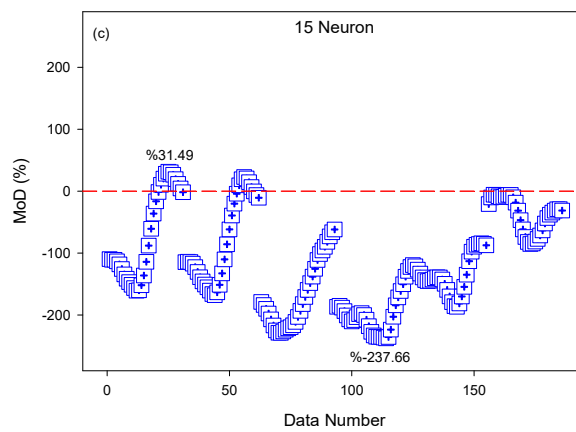


**Figure 9.** Error rates between the data obtained from the ANN model and the target values. (a) 5 neuron (b) 10 neuron (c) 15 neuron.

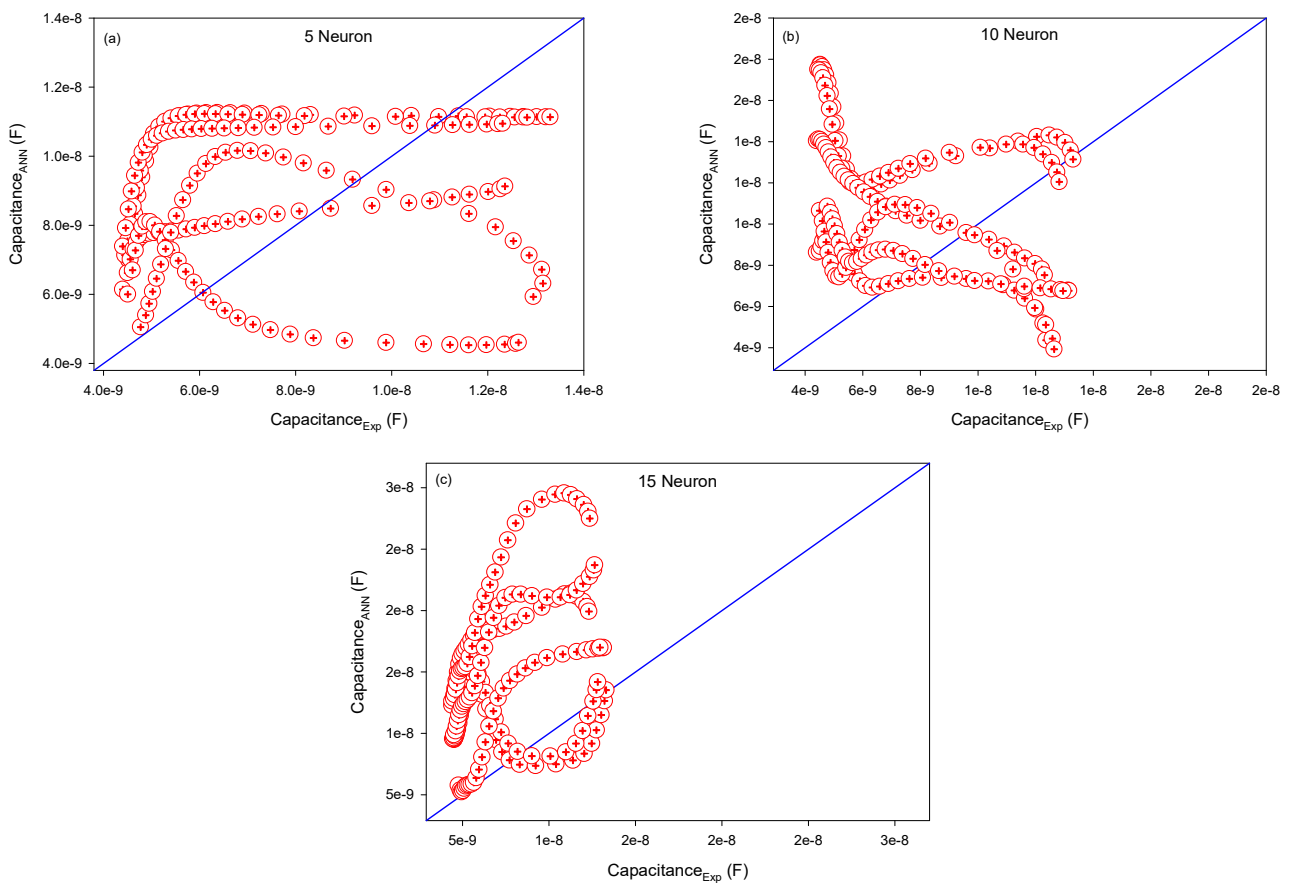


**Figure 10.** Predicted values and target values obtained from ANN model. (a) 5 neuron (b) 10 neuron (c) 15 neuron.

**Table 1.** Performance parameters for the ANN model.

Model	MSE	R	MoD <sub>av</sub> (%)
5 Neuron	$1.39 \times 10^{-17}$	0.09967	-34.92
10 Neuron	$3.66 \times 10^{-17}$	-0.36140	-68.64
15 Neuron	$5.89 \times 10^{-16}$	0.39982	-114.73

It is thought that there are two reasons why the proposed ANN model fails to forecast the capacitance–voltage measurements of the diode with organic polymer interface in this manner, depending on the frequency. The former may be owing to physical reasons, like the conductive polymer layer employed between metal and semiconductor surfaces during manufacturing. The polymer layers utilized at the contact have the potential to impact current conduction [45]. This could have resulted in an inconsistency in the charges, resulting in a capacitive effect on the interface. This imperfection in the contact could have hampered the capacitance–voltage–frequency link. This could have led to the ANN system making inaccurate predictions. The other issue is because the ANN model’s learning method is insufficient to learn material that is irregular and has no relationship, even if it is complex. ANN models are one of the mathematical tools with high predictive ability in modeling complex functions. As can be seen in the comprehensive literature review given, ANNs have been able to offer high prediction performance in many different applications. Another reason for the failure of the models in this study is that the non-functional relationship between the data was not learned enough by the ANN model. As a result of the study, it was seen that the R values obtained from the models were below 0.5. Studies in the literature show that R values are around 0.9. The closeness of the R value to 1 indicates the accuracy of the predicted values obtained from the model. The low R values of the models indicate that the model did not learn enough.

## 6. Conclusions

In the current work, three dissimilar ANN simulations have been constructed to estimate the capacitance voltage productions of a Schottky diode with an organic polymer edge dependent on the frequency. Levenberg–Marquardt procedure has been preferred as the training procedure in MLP networks created with 5, 10, and 15 neurons in the hidden layers. Overall, 130 of the data used in the ANN structures, which have been established using a total of 186 tentative data, have been evaluated in the training of the model, 28 in the validation phase, and 28 in the testing phase. MSE, R, and MoD factors have been evaluated for estimation analysis of ANN structures. The outcomes indicate that the ANN structures have too many deviations and the created ANN structures cannot estimate the capacitance voltage productions of the organic polymer interface Schottky diode dependent on the frequency.

**Author Contributions:** Conceptualization, data curation, methodology, software, writing—original draft: A.B.Ç.; data curation, formal analysis, investigation, validation: T.G.; methodology, validation, writing—review & editing: A.S.; funding acquisition, supervision, writing—review & editing: K.N. All authors have read and agreed to the published version of the manuscript.

**Funding:** This research received no external funding.

**Institutional Review Board Statement:** Not applicable.

**Informed Consent Statement:** Not applicable.

**Data Availability Statement:** The datasets generated during the current study are available from the corresponding author on reasonable request.

**Conflicts of Interest:** The authors declare no conflict of interest.

## References

1. McCulloch, W.S.; Pitts, W. A logical calculus of the ideas immanent in nervous activity. *Bull. Math. Biophys.* **1943**, *5*, 115–133. [[CrossRef](#)]
2. Ding, S.; Li, H.; Su, C.; Yu, J.; Jin, F. Evolutionary artificial neural networks: A review. *Artif. Intell. Rev.* **2013**, *39*, 251–260. [[CrossRef](#)]
3. Tanty, R.; Desmukh, T.S. Application of artificial neural network in hydrology—A review. *Int. J. Eng. Technol. Res.* **2015**, *4*, 184–188.
4. Thakur, N.; Han, C.Y. Indoor Localization for Personalized Ambient Assisted Living of Multiple Users in Multi-Floor Smart Environments. *Big Data Cogn. Comput.* **2021**, *5*, 42. [[CrossRef](#)]

5. Pavićević, M.; Popović, T. Forecasting Day-Ahead Electricity Metrics with Artificial Neural Networks. *Sensors* **2022**, *22*, 1051. [[CrossRef](#)]
6. Yadav, A.K.; Chandel, S. Solar radiation prediction using Artificial Neural Network techniques: A review. *Renew. Sustain. Energy Rev.* **2014**, *33*, 772–781. [[CrossRef](#)]
7. Kumar, R.; Aggarwal, R.; Sharma, J. Energy analysis of a building using artificial neural network: A review. *Energy Build.* **2013**, *65*, 352–358. [[CrossRef](#)]
8. Sharma, P.; Bhatti, T. A review on electrochemical double-layer capacitors. *Energy Convers. Manag.* **2010**, *51*, 2901–2912. [[CrossRef](#)]
9. Rhoderick, E.; Williams, R. *Metal-Semiconductor Contacts*; Clarendon: Oxford, UK, 1988.
10. Liu, Q.; Lau, S. A review of the metal–GaN contact technology. *Solid-State Electron.* **1998**, *42*, 677–691. [[CrossRef](#)]
11. Blom, P.; Wolf, R.; Cillessen, J.; Krijn, M. Ferroelectric schottky diode. *Phys. Rev. Lett.* **1994**, *73*, 2107. [[CrossRef](#)]
12. Rideout, V. A review of the theory, technology and applications of metal-semiconductor rectifiers. *Thin Solid Film.* **1978**, *48*, 261–291. [[CrossRef](#)]
13. Zhao, J.H.; Sheng, K.; Lebron-Velilla, R.C. Silicon carbide schottky barrier diode. *Int. J. High Speed Electron. Syst.* **2005**, *15*, 821–866. [[CrossRef](#)]
14. She, X.; Huang, A.Q.; Lucía, Ó.; Ozpineci, B. Review of silicon carbide power devices and their applications. *IEEE Trans. Ind. Electron.* **2017**, *64*, 8193–8205. [[CrossRef](#)]
15. Wang, X.; Qi, J.; Yang, M.; Zhang, G. Analysis of 600 V/650 V SiC schottky diodes at extremely high temperatures. *CPSS Trans. Power Electron. Appl.* **2020**, *5*, 11–17. [[CrossRef](#)]
16. Lim, S.; Kwon, D.; Eum, J.-H.; Lee, S.-T.; Bae, J.-H.; Kim, H.; Kim, C.-H.; Park, B.-G.; Lee, J.-H. Highly Reliable Inference System of Neural Networks Using Gated Schottky Diodes. *IEEE J. Electron. Devices Soc.* **2019**, *7*, 522–528. [[CrossRef](#)]
17. Rabehi, A.; Nail, B.; Helal, H.; Douara, A.; Ziane, A.; Amrani, M.; Akkal, B.; Benamara, Z. Optimal estimation of Schottky diode parameters using a novel optimization algorithm: Equilibrium optimizer. *Superlattices Microstruct.* **2020**, *146*, 106665. [[CrossRef](#)]
18. Mellit, A.; Sağlam, S.; Kalogirou, S.A. Artificial neural network-based model for estimating the produced power of a photovoltaic module. *Renew. Energy* **2013**, *60*, 71–78. [[CrossRef](#)]
19. Alade, M.O. High Temperature Electronic Properties of a Microwave Frequency Sensor–GaN Schottky Diode. *Adv. Phys. Theor. Appl.* **2013**, *15*, 47–53.
20. Darwish, A.; Hanafy, T.; Attia, A.; Habashy, D.; El-Bakry, M.; El-Nahass, M. Optoelectronic performance and artificial neural networks (ANNs) modeling of n-InSe/p-Si solar cell. *Superlattices Microstruct.* **2015**, *83*, 299–309. [[CrossRef](#)]
21. Mittal, M.; Bora, B.; Saxena, S.; Gaur, A.M. Performance prediction of PV module using electrical equivalent model and artificial neural network. *Sol. Energy* **2018**, *176*, 104–117. [[CrossRef](#)]
22. Liang, A.; Xu, Y.; Jia, S.; Sun, G. Neural networks for nonlinear modeling of microwave Schottky diodes. In Proceedings of the International Conference on Microwave and Millimeter Wave Technology, Nanjing, China, 21–24 April 2008; IEEE: Piscataway, NJ, USA, 2008; pp. 558–561.
23. Torun, Y.; Doğan, H. Modeling of Schottky diode characteristic by machine learning techniques based on experimental data with wide temperature range. *Superlattices Microstruct.* **2021**, *160*, 107062. [[CrossRef](#)]
24. Rahman, A.A.; Zhang, X. Prediction of oscillatory heat transfer coefficient for a thermoacoustic heat exchanger through artificial neural network technique. *Int. J. Heat Mass Transf.* **2018**, *124*, 1088–1096. [[CrossRef](#)]
25. Pang, Z.; Niu, F.; O’Neill, Z. Solar radiation prediction using recurrent neural network and artificial neural network: A case study with comparisons. *Renew. Energy* **2020**, *156*, 279–289. [[CrossRef](#)]
26. Gao, W.; Guirao, J.L.; Basavanagoud, B.; Wu, J. Partial multi-dividing ontology learning algorithm. *Inf. Sci.* **2018**, *467*, 35–58. [[CrossRef](#)]
27. Gao, W.; Wang, W.; Dimitrov, D.; Wang, Y. Nano properties analysis via fourth multiplicative ABC indicator calculating. *Arab. J. Chem.* **2018**, *11*, 793–801. [[CrossRef](#)]
28. Gao, W.; Wu, H.; Siddiqui, M.K.; Baig, A.Q. Study of biological networks using graph theory. *Saudi J. Biol. Sci.* **2018**, *25*, 1212–1219. [[CrossRef](#)]
29. Gao, W.; Guirao, J.L.G.; Abdel-Aty, M.; Xi, W. An independent set degree condition for fractional critical deleted graphs. *Discret. Contin. Dyn. Syst.-S* **2019**, *12*, 877. [[CrossRef](#)]
30. Dimitrov, D.; Abdo, H. Tight independent set neighborhood union condition for fractional critical deleted graphs and ID deleted graphs. *Discret. Contin. Dyn. Syst.-S* **2019**, *12*, 711. [[CrossRef](#)]
31. Bas, E.; Uslu, V.R.; Egrioglu, E. Robust learning algorithm for multiplicative neuron model artificial neural networks. *Expert Syst. Appl.* **2016**, *56*, 80–88. [[CrossRef](#)]
32. Vakili, M.; Khosrojerdi, S.; Aghajannezhad, P.; Yahyaei, M. A hybrid artificial neural network-genetic algorithm modeling approach for viscosity estimation of graphene nanoplatelets nanofluid using experimental data. *Int. Commun. Heat Mass Transf.* **2017**, *82*, 40–48. [[CrossRef](#)]
33. Bahiraei, M.; Heshmatian, S.; Moayedi, H. Artificial intelligence in the field of nanofluids: A review on applications and potential future directions. *Powder Technol.* **2019**, *353*, 276–301. [[CrossRef](#)]
34. Park, J.; Sandberg, I.W. Universal approximation using radial-basis-function networks. *Neural Comput.* **1991**, *3*, 246–257. [[CrossRef](#)] [[PubMed](#)]

35. Valueva, M.V.; Nagornov, N.; Lyakhov, P.A.; Valuev, G.V.; Chervyakov, N.I. Application of the residue number system to reduce hardware costs of the convolutional neural network implementation. *Math. Comput. Simul.* **2020**, *177*, 232–243. [[CrossRef](#)]
36. Garg, S.; Shariff, A.M.; Shaikh, M.S.; Lal, B.; Suleman, H.; Faiqa, N. Experimental data, thermodynamic and neural network modeling of CO<sub>2</sub> solubility in aqueous sodium salt of l-phenylalanine. *J. CO<sub>2</sub> Util.* **2017**, *19*, 146–156. [[CrossRef](#)]
37. Barati-Harooni, A.; Najafi-Marghmaleki, A. An accurate RBF-NN model for estimation of viscosity of nanofluids. *J. Mol. Liq.* **2016**, *224*, 580–588. [[CrossRef](#)]
38. Rostamian, S.H.; Biglari, M.; Saedodin, S.; Esfe, M.H. An inspection of thermal conductivity of CuO-SWCNTs hybrid nanofluid versus temperature and concentration using experimental data, ANN modeling and new correlation. *J. Mol. Liq.* **2017**, *231*, 364–369. [[CrossRef](#)]
39. Esmaeilzadeh, F.; Teja, A.S.; Bakhtyari, A. The thermal conductivity, viscosity, and cloud points of bentonite nanofluids with n-pentadecane as the base fluid. *J. Mol. Liq.* **2020**, *300*, 112307. [[CrossRef](#)]
40. Bonakdari, H.; Zaji, A.H. Open channel junction velocity prediction by using a hybrid self-neuron adjustable artificial neural network. *Flow Meas. Instrum.* **2016**, *49*, 46–51. [[CrossRef](#)]
41. Ahmadloo, E.; Azizi, S. Prediction of thermal conductivity of various nanofluids using artificial neural network. *Int. Commun. Heat Mass Transf.* **2016**, *74*, 69–75. [[CrossRef](#)]
42. Wang, J.; Ayari, M.A.; Khandakar, A.; Chowdhury, M.E.H.; Zaman, S.M.U.; Rahman, T.; Vaferi, B. Estimating the Relative Crystallinity of Biodegradable Polylactic Acid and Polyglycolide Polymer Composites by Machine Learning Methodologies. *Polymers* **2022**, *14*, 527. [[CrossRef](#)]
43. Gunduz, B.; Yahia, I.; Yakuphanoglu, F. Electrical and photoconductivity properties of p-Si/P3HT/Al and p-Si/P3HT: MEH-PPV/Al organic devices: Comparison study. *Microelectron. Eng.* **2012**, *98*, 41–57. [[CrossRef](#)]
44. Reddy, V.R. Electrical properties of Au/polyvinylidene fluoride/n-InP Schottky diode with polymer interlayer. *Thin Solid Film.* **2014**, *556*, 300–306. [[CrossRef](#)]
45. Forrest, S.; Schmidt, P. Semiconductor analysis using organic-on-inorganic contact barriers. I. Theory of the effects of surface states on diode potential and ac admittance. *J. Appl. Phys.* **1986**, *59*, 513–525. [[CrossRef](#)]